

Accepted Manuscript

Xanthenes and sesquiterpene derivatives from a marine-derived fungus
Scopulariopsis sp.

Mohamed S. Elnaggar, Sherif S. Ebada, Mohamed L. Ashour, Weaam Ebrahim,
Werner E.G. Müller, Attila Mándi, Tibor Kurtán, Abdelnasser Singab, Wenhan Lin,
Zhen Liu, Peter Proksch

PII: S0040-4020(16)30192-2

DOI: [10.1016/j.tet.2016.03.073](https://doi.org/10.1016/j.tet.2016.03.073)

Reference: TET 27613

To appear in: *Tetrahedron*

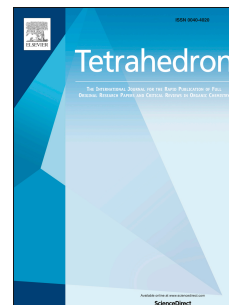
Received Date: 21 December 2015

Revised Date: 7 March 2016

Accepted Date: 17 March 2016

Please cite this article as: Elnaggar MS, Ebada SS, Ashour ML, Ebrahim W, Müller WEG, Mándi A, Kurtán T, Singab A, Lin W, Liu Z, Proksch P, Xanthenes and sesquiterpene derivatives from a marine-derived fungus *Scopulariopsis* sp., *Tetrahedron* (2016), doi: 10.1016/j.tet.2016.03.073.

This is a PDF file of an unedited manuscript that has been accepted for publication. As a service to our customers we are providing this early version of the manuscript. The manuscript will undergo copyediting, typesetting, and review of the resulting proof before it is published in its final form. Please note that during the production process errors may be discovered which could affect the content, and all legal disclaimers that apply to the journal pertain.

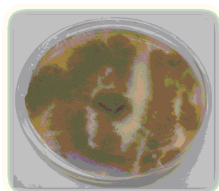
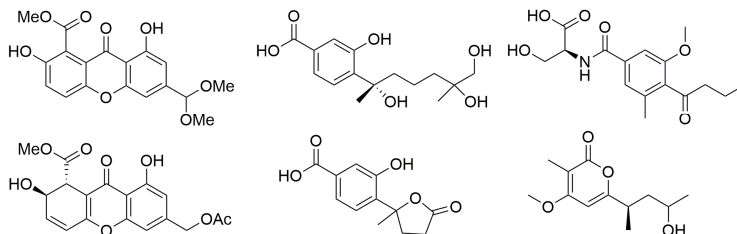


Graphical Abstract

Xanthenes and sesquiterpene derivatives from a marine-derived fungus *Scopulariopsis* sp.

Leave this area blank for abstract info.

Mohamed S. Elnaggar, Sherif S. Ebada, Mohamed L. Ashour, Weam Ebrahim, Werner E. G. Müller, Attila Mándi, Tibor Kurtán, Abdelnasser Singab, Wenhan Lin, Zhen Liu, and Peter Proksch

*Scopulariopsis* sp.

Xanthenes and sesquiterpene derivatives from a marine-derived fungus *Scopulariopsis* sp.

Mohamed S. Elnaggar,^{a,b} Sherif S. Ebada,^b Mohamed L. Ashour,^b Weam Ebrahim,^{a,c} Werner E. G. Müller,^d Attila Mándi,^e Tibor Kurtán,^e Abdelnasser Singab,^b Wenhan Lin,^f Zhen Liu,^{a,*} and Peter Proksch^{a,*}

^a *Institute of Pharmaceutical Biology and Biotechnology, Heinrich-Heine-Universität Düsseldorf, Universitätsstrasse 1, 40225 Düsseldorf, Germany*

^b *Department of Pharmacognosy, Faculty of Pharmacy, Ain-Shams University, Abbassia, Cairo 11566, Egypt*

^c *Department of Pharmacognosy, Faculty of Pharmacy, Mansoura University, Mansoura 35516, Egypt*

^d *Institut für Physiologische Chemie, Universitätsmedizin der Johannes Gutenberg-Universität Mainz, Duesbergweg 6, 55128 Mainz, Germany*

^e *Department of Organic Chemistry, University of Debrecen, P. O. B. 20, 4010 Debrecen, Hungary*

^f *State Key Laboratory of Natural and Biomimetic Drugs, Peking University, 100191 Beijing, China*

*Corresponding authors.

Tel.: +49 211 81 14163; fax: +49 211 81 11923;

e-mail: zhenfeizi0@sina.com (Z. Liu),

proksch@uni-duesseldorf.de (P. Proksch)

Abstract:

Two new xanthone derivatives, 12-dimethoxypinselin (**1**) and 12-*O*-acetyl-AGI-B4 (**2**), as well as two new phenolic bisabolane-type sesquiterpenes, 11,12-dihydroxysydonic acid (**15**) and 1-hydroxyboivinianic acid (**16**), together with one new alkaloid, scopulamide (**21**) and one new α -pyrone derivative, scopupyrone (**26**), in addition to twenty-three known compounds (**3–14**, **17–20**, **22–25**, **27–29**) were isolated from solid rice cultures of the marine-derived fungus *Scopulariopsis* sp. obtained from the Red Sea hard coral *Stylophora* sp. All compounds were unambiguously identified through extensive NMR spectroscopic analyses, and by comparison with the literature. Marfey's reaction was performed to determine the absolute configuration of scopulamide (**21**) and TDDFT-ECD calculations were used to assign the configuration of AGI-B4 (**3**) and scopupyrone (**26**). All isolated compounds were evaluated for their cytotoxicity against L5178Y mouse lymphoma cells and the structure-activity relationships were discussed.

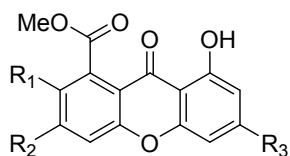
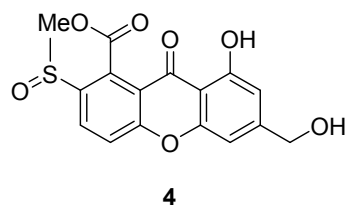
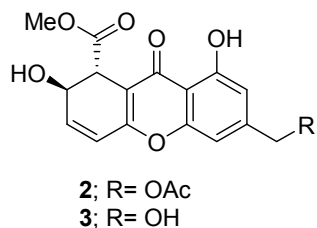
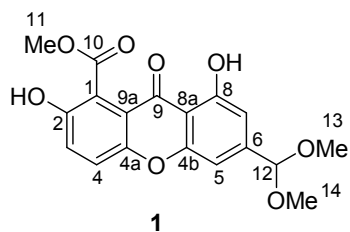
Keywords: *Scopulariopsis* sp.; Xanthone; Sesquiterpene; Structural elucidation; Cytotoxicity

1. Introduction

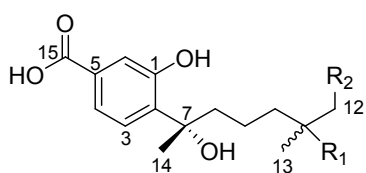
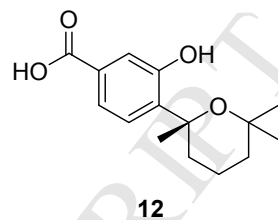
Marine microorganisms have been recognized as an important source of bioactive secondary metabolites.¹ For example, phomactins,² a class of fungal diterpenoids, which were initially found in the fungus *Phoma* sp. obtained from the shell of the crab *Chionoecetes opilio*, attracted attention due to their pronounced platelet activating factor antagonizing activity. Moreover, peribysins³ isolated from the sea hare-derived fungus *Periconia byssoides* are well-known as cell-adhesion inhibitors, and tryptostatins,⁴ structurally unique indole alkaloids, which were firstly isolated from *Aspergillus fumigatus*, a fungus obtained from a sea sediment sample, exhibit mammalian cell cycle inhibition activity. In addition, some of these metabolites have advanced to clinical trials and may potentially be launched as pharmaceutical drugs in the future. One of the most prominent examples of fungal derived bioactive compounds is plinabulin (NPI-2358), a synthetic analogue of the diketopiperazine alkaloid halimide which is produced by *Aspergillus* sp. CNC-139 isolated from the alga *Halimeda lacrimosa*. Plinabulin acts as a vascular disrupting agent (VDA) and inhibits tubulin polymerization, resulting in selective collapse of tumor endothelial vasculature. It is currently undergoing phase II clinical trials for patients with advanced non-small-cell lung cancer.⁵

In continuation of our ongoing efforts to identify new fungal products from rare and unusual niches,⁶⁻¹¹ we investigated the marine-derived fungus *Scopulariopsis* sp., which was isolated from the inner tissues of the Red Sea hard coral *Stylophora* sp. collected in Egypt. The ethyl acetate extract of this fungus when grown on solid rice medium was found to exhibit cytotoxicity against the mouse lymphoma cell line L5178Y in a preliminary bioassay. Moreover, a literature survey revealed that chemical studies on fungi of this genus have rarely been conducted. So far two

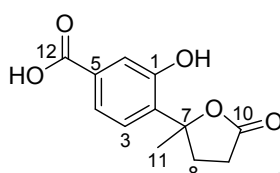
cytotoxic cyclodepsipeptides,¹² two naphthalene derivatives,¹³ and one alkaloid named fumiquinazoline L¹⁴ had been reported. In the present study, 29 compounds including 11 xanthenes (**1–11**), 5 sesquiterpene derivatives (**12–16**), 4 phenyl ethers (**17–20**), 5 alkaloids (**21–25**), and 4 miscellaneous compounds (**26–29**) were isolated from solid rice cultures of *Scopulariopsis* sp.. Among them, 12-dimethoxypinselin (**1**), 12-*O*-acetyl-AGI-B4 (**2**), 11,12-dihydroxysydonic acid (**15**), 1-hydroxyboivinianic acid (**16**), scopulamide (**21**) and scopupyrone (**26**) are new natural products. Besides, sydownin B (**6**) and 11-hydroxysydonic acid (**14**) were also isolated from the host coral *Stylophora* sp. in this study. Herein, we describe the isolation, structural elucidation and cytotoxic activity of the compounds obtained.



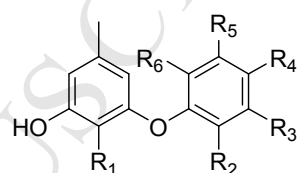
- 5**; R₁ = OH, R₂ = H, R₃ = CH₃
6; R₁ = OH, R₂ = H, R₃ = CH₂OH
7; R₁ = OH, R₂ = H, R₃ = CH₂OAc
8; R₁ = OH, R₂ = H, R₃ = COOH
9; R₁ = H, R₂ = H, R₃ = CH₂OH
10; R₁ = H, R₂ = H, R₃ = COOH
11; R₁ = H, R₂ = OH, R₃ = CH₃



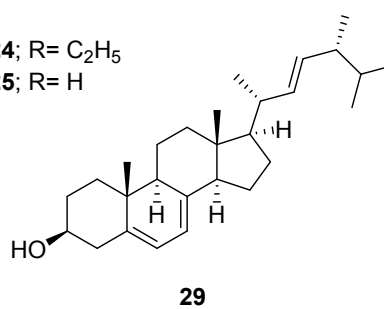
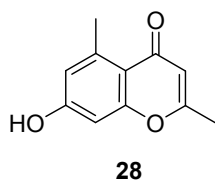
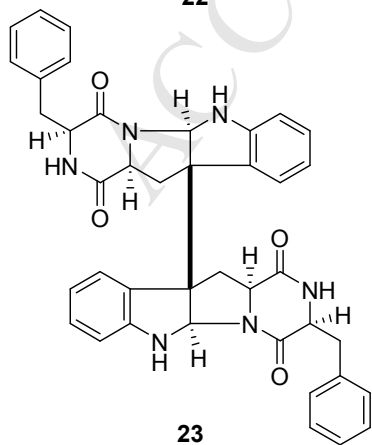
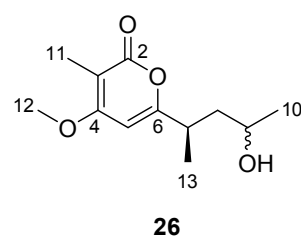
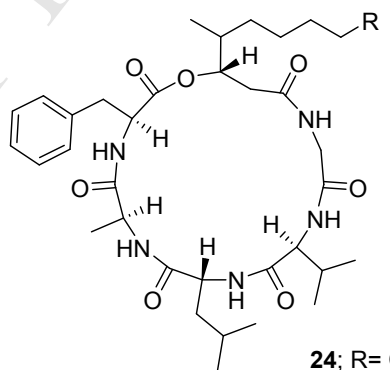
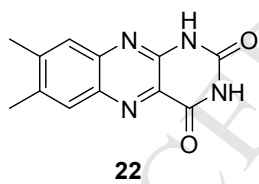
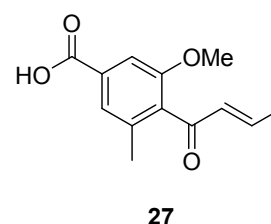
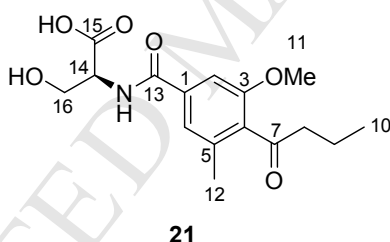
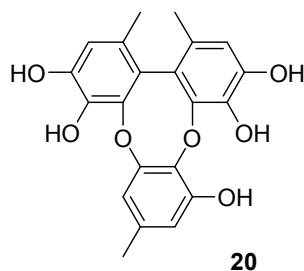
- 13**; R₁ = H, R₂ = H
14; R₁ = OH, R₂ = H
15; R₁ = OH, R₂ = OH



16



- 17**; R₁, R₂, R₃ = OH, R₄, R₆ = H, R₅ = CH₃
18; R₁, R₂, R₆ = OH, R₃, R₅ = H, R₄ = CH₃
19; R₁, R₂, R₄, R₆ = H, R₃ = OH, R₅ = CH₃



2. Results and discussion

Scopulariopsis sp. was grown on solid rice medium and subsequently extracted with EtOAc, followed by partitioning of the dried extract between *n*-hexane and 90% aqueous MeOH. The resulting aqueous MeOH phase was fractionated by repeated column chromatography over silica gel, Sephadex LH-20, followed by semi-preparative HPLC to afford compounds **1-29**.

Compound **1** was isolated as a pale yellow solid. The molecular formula was determined as C₁₈H₁₆O₈, based on the pseudomolecular ion peak of [M+H]⁺ at *m/z* 361.0915, indicating 11 degrees of unsaturation. Its UV spectrum, which displayed absorption bands at λ_{\max} 203, 237, 265 and 380 nm, was similar to that of pinselin (**5**),¹⁵ suggesting that both compounds share the same core structure. The ¹H NMR spectrum of **1** (Table 1) exhibited four aromatic protons at δ_{H} 7.51 (1H, d, *J* = 9.1 Hz), 7.36 (1H, d, *J* = 9.1 Hz), 7.06 (1H, br s), and 6.81 (1H, br s), three methoxy groups at δ_{H} 3.97 (3H, s) and 3.36 (6H, s), and an oxygenated methine at δ_{H} 5.42 (1H, s). Meanwhile, ¹³C NMR data (Table 1) along with HSQC and HMBC spectral analysis revealed the presence of 18 carbons, including one chelated carbonyl group (δ_{C} 181.2), one carboxyl group (δ_{C} 170.2), eight quaternary carbons (δ_{C} 162.3, 157.1, 154.3, 150.1, 136.7, 118.8, 118.4, and 109.4), five tertiary carbons (δ_{C} 127.1, 120.8, 108.9, 106.1, and 103.1), and three methoxy groups (δ_{C} 53.1, 53.1, and 52.9). These NMR data were comparable to those of pinselin (**5**)¹⁵ except for the replacement of the aromatic methyl substituent by an additional oxygenated methine (δ_{C} 103.1, δ_{H} 5.42) and the appearance of two additional methoxy groups (δ_{C} 53.1, δ_{H} 3.36). In the HMBC spectrum of **1**, H-5 (δ_{H} 7.06) and H-7 (δ_{H} 6.81) exhibited correlations to the carbon of the additional oxygenated methine (C-12), while the latter proton displayed correlations to C-5 (δ_{C} 106.1) and C-7 (δ_{C} 108.9) respectively, supporting the

assignment of the oxygenated methine at C-12. Besides, the HMBC correlations from the protons of the two additional methoxy groups to C-12 indicated their linkage at C-12. The gross structure of **1** was further confirmed by detailed examination of COSY and HMBC spectra (Figure 1). Hence, compound **1** was elucidated as 12-dimethoxypinselin.

Table 1. NMR Data for Compounds **1** and **2** (^1H at 600 MHz, ^{13}C at 150 MHz)

position	1 ^a		2 ^b	
	δ_{C}	δ_{H} (J in Hz)	δ_{C}	δ_{H} (J in Hz)
1	118.4, C		45.4, CH	4.18, d (3.2)
2	154.3, C		64.8, CH	4.76, m
3	127.1, CH	7.36, d (9.1)	141.3, CH	6.75, dd (9.9, 4.9)
4	120.8, CH	7.51, d (9.1)	122.3, CH	6.53, d (9.9)
4a	150.1, C		161.0, C	
4b	157.1, C		156.4, C	
5	106.1, CH	7.06, br s	106.0, CH	7.04, br s
6	136.7, C		146.5, C	
7	108.9, CH	6.81, br s	110.3, CH	6.81, br s
8	162.3, C		161.3, C	
8a	109.4, C		110.4, C	
9	182.5, C		183.0, C	
9a	118.8, C		111.6, C	
10	170.3, C		171.3, C	
11	52.9, CH ₃	3.97, s	52.9, CH ₃	3.66, s
12	103.1, CH	5.42, s	65.3, CH ₂	5.18, s
13	53.1, CH ₃	3.36, s	170.6, C	
14	53.1, CH ₃	3.36, s	20.3, CH ₃	2.13, s
8-OH				12.61, s

^a Spectra recorded in CD₃OD. ^b Spectra recorded in CD₃COCD₃.

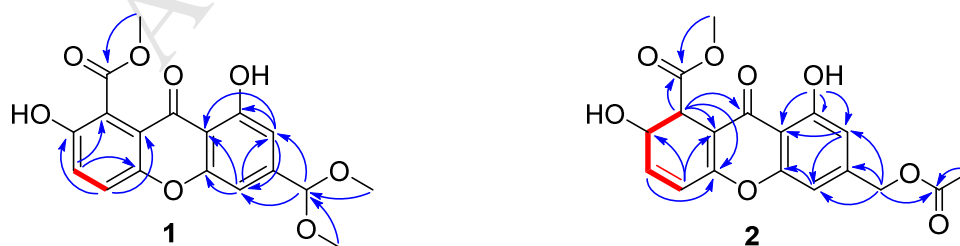


Figure 1. Key COSY (bold lines) and HMBC (arrows) correlations of compounds **1** and **2**.

Compound **2** was obtained as a yellow solid and its UV spectrum was almost identical to that of AGI-B4 (**3**)¹⁶. The molecular formula of **2** was determined as C₁₈H₁₆O₈ by HRESIMS, indicating 42 additional amu compared to **3**. Comparison of the NMR data (Table 1) with those of **3** revealed that the two compounds were structurally similar, except for the presence of an additional acetyl group in **2** as evident from the signals at δ_C 170.6 (qC) and 20.3 (CH₃) in the ¹³C NMR and the corresponding signal at δ_H 2.13 (3H, s) in the ¹H NMR spectrum. The location of this acetyl group at C-12 was confirmed by the HMBC correlation from H-12 (δ_H 5.18, s) to the acetyl carbonyl carbon. The relative configuration of **2** was deduced from the coupling constant (³J_{1,2} = 3.2 Hz), which is similar to that of **3** (³J_{1,2} = 3.7 Hz). Thus compound **2** was identified as the 12-*O*-acetyl-AGI-B4. The ECD spectrum of **2** showed a baseline curve, which considering the chiral dihydroxanthone chromophore, suggested that **2** was either a racemate or it had a low enantiomeric excess. This was confirmed by chiral HPLC analysis using Chiralpack IA column, which showed 17% enantiomeric excess of **2**. In contrast, the related derivative **3** gave a distinct ECD spectrum and its specific rotation, $[\alpha]_D^{20}$ -28.0 (*c* 0.40, MeOH) was found much larger than the reported value $[\alpha]_D^{20}$ -1.6 (*c* 0.4, MeOH).¹⁶ According to these results, it is probable that the reported sample with -1.6 specific rotation was a racemic mixture or it had very low enantiomeric excess. Meanwhile, chiral HPLC analysis for compound **3** showed that it had 70% enantiomeric excess.

Although the relative configuration of **3** was determined by X-ray analysis,¹⁶ its absolute configuration has not been reported yet. The solution TDDFT-ECD calculation protocol was applied to determine the absolute configuration of **3**. ECD calculations were performed on the arbitrarily chosen (1*R*,2*R*)-enantiomer of **3**. The initial MMFF conformational search yielded 24 conformers in a 21 kJ/mol energy

window, the B3LYP/6-31G(d) *in vacuo* reoptimization of which resulted in 10 low-energy ($\geq 2\%$) conformers (Figure 2). In all the ten low-energy conformers, the C-1 methoxycarbonyl and 2-hydroxyl groups adopted *axial* orientation, which was in agreement with the measured small value of the $^3J_{1,2}$ coupling constant. The $\omega_{C-3,C-4,C-4a,C-9a}$ torsional angle had a negative value for all the conformers with values between -9° and -11° . The structures of conformers differed in the orientation of the methoxycarbonyl group and the proton of the 2- and 12-hydroxyl groups. Boltzmann-averaged ECD spectra calculated for the above conformers at various levels (B3LYP/TZVP, BH&HLYP/TZVP and PBE0/TZVP) reproduced well the experimental spectrum with BH&HLYP/TZVP giving the best agreement (Figure 3). Since all the applied theoretical levels and all the low-energy conformers gave similar and consistent results, the absolute configuration of **3** could be unambiguously determined as 1*R*, 2*R*.

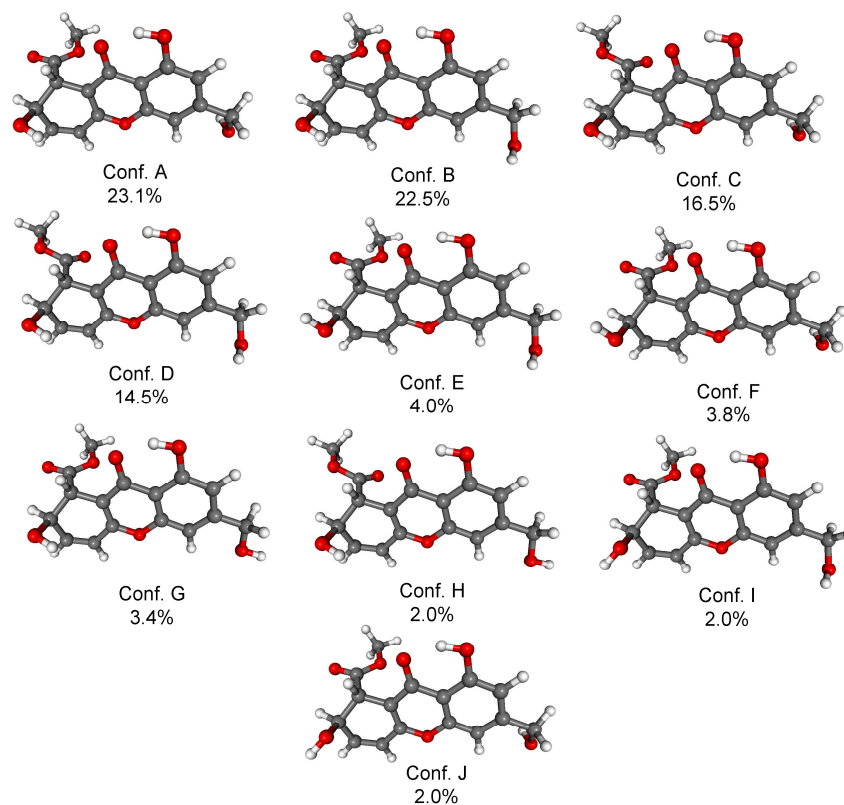


Figure 2. Structures and populations of the low-energy B3LYP/6-31G(d) conformers ($\geq 2\%$) of (1*R*,2*R*)-**3**.

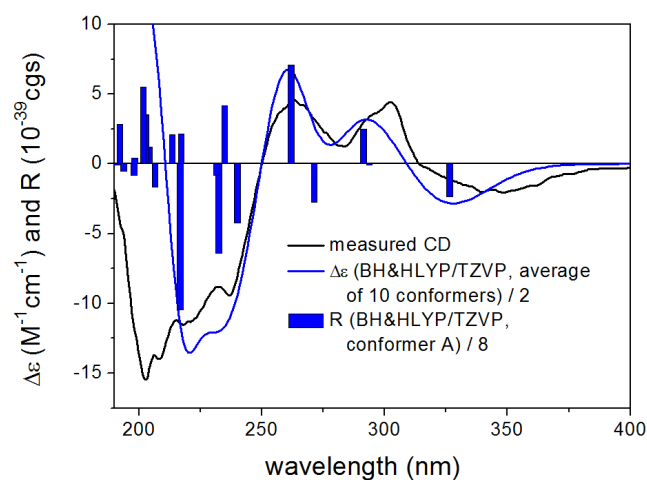


Figure 3. Experimental ECD spectrum of (-)-**3** in MeCN compared with the Boltzmann-weighted BH&HLYP/TZVP ECD spectrum of (1*R*,2*R*)-**3** computed for the B3LYP/6-31G(d) *in vacuo* conformers. Bars represent the rotational strength of the lowest-energy conformer.

Compound **15** was obtained as a white amorphous powder, with $[\alpha]_D^{20}$ of + 4.3 (*c* 0.23, MeOH). The UV spectrum showed absorption maxima at 220, 246 and 302 nm, and resembles that of sydonic acid (**13**)¹⁷ and 11-hydroxysydonic acid (**14**)¹⁸. Its molecular formula was determined as C₁₅H₂₂O₆ by HRESIMS, containing one additional oxygen atom compared to **14**. The NMR data (Table 2) of **15** were comparable to those of **14**, except for the appearance of the signals of a hydroxymethyl substituent (δ_C 69.8, δ_H 3.28) in **15**, instead of the signals for a methyl group (δ_C 29.6, δ_H 1.10) in **14**. The HMBC correlations from the protons of this hydroxymethyl group to C-10 (δ_C 39.3), C-11 (δ_C 72.1) and C-13 (δ_C 23.8) indicated the hydroxymethyl substituent of **15** to be present at C-12. Analysis of the COSY and HMBC spectra (Figure 4) confirmed the planar structure of **15**. The absolute configuration at C-7 in **15** was determined as *S*, due to the similarity of the ECD spectrum compared with (*S*)-sydonol.¹⁷ Attempts to determine the absolute

configuration at C-11 using the modified Mosher's method were unsuccessful due to the limited amount of the sample.

Table 2. NMR Data for Compounds **15** and **16** (^1H at 600 MHz, ^{13}C at 150 MHz)

position	15 ^a		16 ^b	
	δ_{C}	δ_{H} (J in Hz)	δ_{C}	δ_{H} (J in Hz)
1	157.0, C		154.2, C	
2	136.3, C		135.9, C	
3	127.4, CH	7.27, d (8.1)	125.6, CH	7.39, d (7.8)
4	120.7, CH	7.45, dd (8.1,1.7)	121.4, CH	7.48, m
5	130.9, C		133.5, C	
6	118.3, CH	7.39, d (1.7)	117.8, CH	7.47, m
7	78.2, C		88.3, C	
8	44.0, CH ₂	1.99, m	34.7, CH ₂	2.69, m
		1.84, m		2.53, m
9	18.5, CH ₂	1.47, m	29.3, CH ₂	2.67, m
		1.41, m		2.46, m
10	39.3, CH ₂	1.42, m	179.5, C	
11	72.1, C		26.2, CH ₃	1.78, s
12	69.8, CH ₂	3.28, br s	170.3, C	
13	23.8, CH ₃	1.04, br s		
14	29.0, CH ₃	1.66, s		
15	167.0, C			

^a Spectra recorded in CD_3COCD_3 . ^b Spectra recorded in CD_3OD .

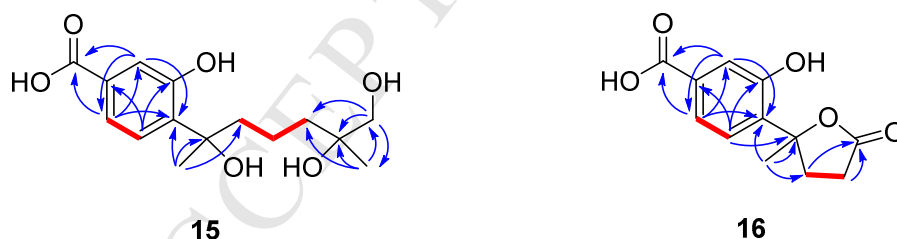


Figure 4. Key COSY (bold lines) and HMBC (arrows) correlations of compounds **15** and **16**.

The molecular formula of compound **16** was established as $\text{C}_{12}\text{H}_{12}\text{O}_5$, implying seven degrees of unsaturation. The 1D and 2D NMR data indicated the gross structure of **16** to be similar to that of 1-hydroxyboivinianin A,¹⁹ except for the replacement of an aromatic methyl substituent by a carboxyl substituent. This was evident from the C-12 resonance (δ_{C} 170.3) and the HMBC correlations from H-4 (δ_{H} 7.48) and H-6

(δ_{H} 7.47) to it. Therefore, **16** was identified as 1-hydroxyboivinianic acid. The ECD spectrum of **16** was a baseline curve, which proved that it was a racemic mixture.

Scopulamide (**21**) was recovered as a yellow amorphous powder, and its molecular formula was determined as $\text{C}_{16}\text{H}_{21}\text{NO}_6$ based on HRESIMS data ($[\text{M}+\text{H}]^+$ at m/z 324.1438, calcd. 324.1447), indicating seven degrees of unsaturation. The UV spectrum exhibited absorption maxima at 205, 251 and 299 nm, which is similar to that of pyrenochaetic acid derivatives.²⁰ The ^1H NMR spectrum (Table 3) of **21** revealed the presence of three methyl groups, including an aliphatic methyl signal at δ_{H} 0.96 (3H, t, $J=7.3$ Hz, H₃-10), an aromatic methyl signal at δ_{H} 2.21 (3H, s, H₃-12), and a methoxy signal at δ_{H} 3.89 (3H, s, H₃-11). Besides, two methylene signals at δ_{H} 2.74 (2H, t, $J=7.3$ Hz, H₂-8) and δ_{H} 1.66 (2H, sext, $J=7.3$ Hz, H₂-9), as well as two aromatic protons located at δ_{H} 7.44 (1H, br s, H-2) and 7.42 (1H, br s, H-6) were found. Upon comparing these data with the literature, it was clear that a partial structure of **21** is in accordance with that of pyrenochaetic acid C,²⁰ which was confirmed by analysis of 2D NMR spectra (Figure 5). In the HMBC spectrum of **21**, H-2 showed a correlation to C-6 (δ_{C} 122.2), H-6 showed a correlation to C-2 (δ_{C} 108.5), and both H-2 and H-6 exhibited correlations to C-4 (δ_{C} 135.0) and C-13 (δ_{C} 166.7), while H₃-12 displayed correlations to C-4, C-5 (δ_{C} 135.8) and C-6, and H₃-11 exhibited correlations to C-3 (δ_{C} 157.2). In addition, the COSY correlations between H₂-8 and H₂-9 and in turn between H₂-9 and H₃-10, as well as the HMBC correlations from H₂-8 and H₂-9 to C-7 (δ_{C} 206.7) were observed. These findings supported a 1,3,4,5-tetrasubstituted benzene ring with a carboxyl group at C-1, a methoxy group at C-3, a propyl side chain moiety at C-4, and a methyl group at C-5. Apart from these signals, a hydroxymethylene group (δ_{C} 62.5, δ_{H} 4.03 and 3.96, CH₂-16), a methine (δ_{C} 56.1, δ_{H} 4.73, CH-14), and an amide proton (δ_{H} 7.86, NH) were observed. The COSY

correlations between H₂-16/H-14 and H-14/NH, as well as the weak NOE correlations from NH to H-2 and H-6, combined with its molecular formula, indicated the presence of a serine moiety linked to the carboxyl group via an amide bond. In order to determine the absolute configuration of **21**, acid hydrolysis followed by subsequent derivatization of the liberated serine moiety using Marfey's method²¹ were conducted. Comparison of the retention time (using LCMS) of the resulting product with those of L- and D-serine that were available as authentic standards and that were subjected to the same treatment as **21**, revealed the presence of L-serine in **21**. Consequently, scopulamide (**21**) was determined as pyrenochaetic acid C connected to an L-serine amino acid moiety through an amide linkage. This is the first report of an *N*-containing pyrenochaetic acid derivative.

Table 3. NMR Data for Compounds **21** and **26** (¹H at 600 MHz, ¹³C at 150 MHz)

position	21 ^a		26 ^b	
	δ_C	δ_H (J in Hz)	δ_C	δ_H (J in Hz)
1	not detected			
2	108.5, CH	7.44, br s	167.8, C	
3	157.2, C		100.9, C	
4	135.0, C		168.8, C	
5	135.8, C		96.0, CH	6.45, s
6	122.2, CH	7.42, br s	168.6, C	
7	206.7, C		36.7, CH	2.93, m
8	46.4, CH ₂	2.74, t (7.3)	44.5, CH ₂	1.81, m 1.57, m
9	17.3, CH ₂	1.66, sext (7.3)	65.8, CH	3.57, m
10	13.7, CH ₃	0.96, t (7.3)	23.8, CH ₃	1.15, d (6.2)
11	56.0, CH ₃	3.89, s	8.1, CH ₃	1.86, s
12	18.6, CH ₃	2.21, s	57.0, CH ₃	3.95, s
13	166.7, C		19.3, CH ₃	1.26, d (7.0)
14	56.1, CH	4.73, m		
15	not detected			
16	62.5, CH ₂	4.03, m 3.96, m		
NH		7.86, br s		

^a Spectra recorded in CD₃COCD₃. ^b Spectra recorded in CD₃OD.

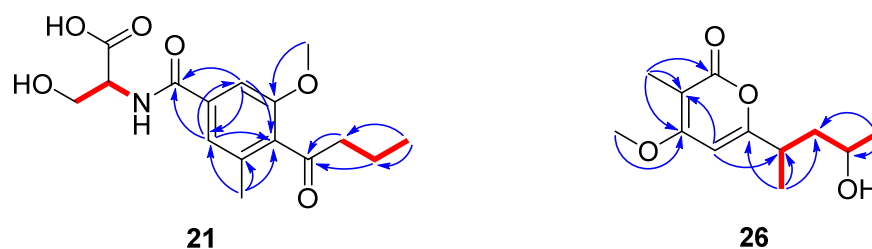


Figure 5. Key COSY (bold lines) and HMBC (arrows) correlations of compounds **21** and **26**.

Compound **26** exhibited absorption maxima at 205 and 300 nm in the UV spectrum, suggesting the presence of an α -pyrone moiety.²² The HRESIMS data supported the molecular formula C₁₂H₁₈O₄, indicating four degrees of unsaturation. Analysis of the ¹H NMR data (Table 3), showed the presence of one methoxy group at δ_{H} 3.95 (3H, s, H₃-12), three methyl groups at δ_{H} 1.15 (3H, d, J = 6.2 Hz, H₃-10), 1.26 (3H, d, J = 7.0 Hz, H₃-13) and 1.86 (3H, s, H₃-11), one methylene group at δ_{H} 1.57 and 1.81 (1H, m, each, H₂-8), and three methine protons at δ_{H} 6.45 (1H, s, H-5, aromatic), 3.57 (1H, m, H-9, oxygenated), and 2.93 (1H, m, H-7). The COSY correlations between H₃-13/H-7, H-7/H₂-8, H₂-8/H-9, and H-9/H₃-10, as well as the HMBC correlations from H₃-10 to C-8 (δ_{C} 44.5) and C-9 (δ_{C} 65.8), and from H₃-13 to C-7 (δ_{C} 36.7) and C-8 indicated that a 1-methyl-3-hydroxybut-1-yl group was present in **26**. Furthermore, key HMBC correlations from H₃-11 to C-2 (δ_{C} 167.8), C-3 (δ_{C} 100.9), and C-4 (δ_{C} 168.8), from H₃-12 to C-4, from H-5 to C-3 and C-7, and from H₃-13 to C-6 (δ_{C} 168.6) confirmed the presence of α -pyrone nucleus and the attachment of methyl, methoxy and 1-methyl-3-hydroxybutyl groups at C-3, 4, and 6 positions, respectively. Thus, the structure of **26** was confirmed as a new natural product for which the name scopupyrone is proposed. Due to the conformational flexibility of the side-chain, the relative configuration of the two stereogenic centers could not be determined by NMR. The ECD features are governed primarily by the C-

7 stereogenic center attached directly to the 2*H*-pyran-2-one chromophore, while the C-9 stereogenic center is expected to have only negligible contribution.

For the configurational assignment of C-7 in **26**, the TDDFT-ECD spectrum was calculated for the solution conformers of the arbitrarily chosen (7*S*,9*R*)-**26**. The B3LYP/6-31G(d) *in vacuo* reoptimization of the 123 MMFF conformers of (7*S*,9*R*)-**26** resulted in 8 low-energy conformers above 2% (Figure 6).

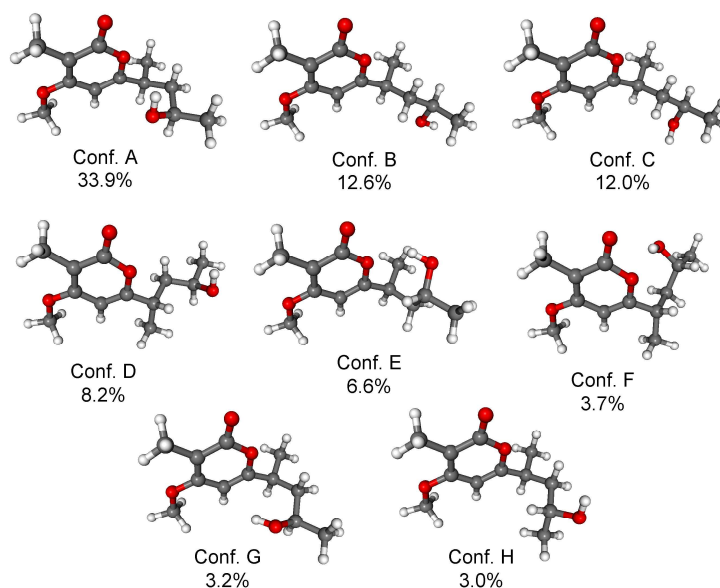


Figure 6. Structures and populations of the low-energy *in vacuo* B3LYP/6-31G(d) conformers ($\geq 2\%$) of (7*S*,9*R*)-**26**.

The computed conformers differed in the conformation of the 1-methyl-3-hydroxybut-1-yl side-chain. Since the C-7 stereogenic center of **26** is contiguous to the achiral 2*H*-pyran-2-one chromophore, the conformation of the side-chain and especially the $\omega_{\text{H-7,C-7,C-6,C-5}}$ torsional angle is decisive for the ECD spectrum. In the lowest-energy conformer (conf A, 33.9%), the C-7–H-7 bond was nearly *cis-co-planar* with the C-5–H-5 bond with -16.4° for the $\omega_{\text{H-7,C-7,C-6,C-5}}$ torsional angle. Similar *cis-co-planar* conformation is represented by conformers B, C, E, G and H with $+0.8^\circ$, -1.5° , $+7.9^\circ$, $+1.0^\circ$ and -5.6° $\omega_{\text{H-7,C-7,C-6,C-5}}$ torsional angles totalling

37.4% population, respectively. In conformers D and F, C-13 was nearly *syn-co-planar* with H-5 resulting in -129.8° and -142.0° $\omega_{\text{H-7,C-7,C-6,C-5}}$ torsional angles with a total population of 11.9%. The ECD spectra computed for the different conformers reflected well the differences of the $\omega_{\text{H-7,C-7,C-6,C-5}}$ torsional angles; the C-7–H-7 *syn-co-planar* conformers (conf A, B, C, E, G and H) had mirror image ECD curves of the experimental spectrum, while two major ECD transitions inverted signs in the computed ECD of conformers D and F and hence they were quite similar to the experimental ones (Figure 7).

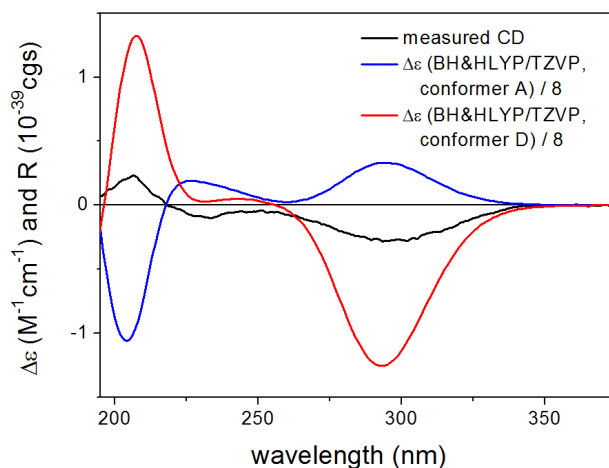


Figure 7. Experimental ECD spectrum of **26** in MeCN compared with the computed BH&HLYP/TZVP ECD spectra of the *in vacuo* B3LYP/6-31G(d) conformers A (blue) and D (red) of (7*S*,9*R*)-**26**.

The Boltzmann-weighted computed ECD spectra of (7*S*,9*R*)-**26** gave mirror image curves of the experimental spectrum with all the three methods tested (Figure 8), which clearly suggested 7*R* absolute configuration for **26**. The absolute configuration of the C-9 stereogenic center cannot be determined by ECD calculations.

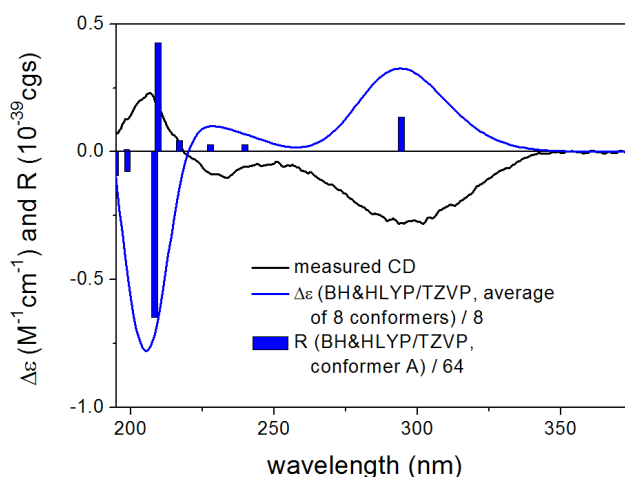


Figure 8. Experimental ECD spectrum of **26** in MeCN compared with the Boltzmann-weighted BH&HLYP/TZVP ECD spectrum of (7*S*,9*R*)-**26** computed for the B3LYP/6-31G(d) *in vacuo* conformers. Bars represent the rotational strength of the lowest-energy conformer.

Due to the presence of the low-energy conformer D and F having opposite ECD curves, the reliability of our ECD calculation greatly depends on the proper estimation of population for the two types of conformation. Thus we thought it was necessary to confirm the above results by applying a newer functional, larger basis set and PCM solvent model.^{23,24}

Reoptimization of the MMFF conformers was repeated at B97D/TZVP PCM/MeCN level^{23,25} affording 14 conformers above 2% population (Figure S37). Similarly to the previous *in vacuo* calculation, the C-7–H-7 *syn-co-planar* conformers were found the major ones represented by 9 conformers with a total population of 59.0%, while the C-13–H-5 *syn-co-planar* conformers had 15.1% total population from 5 minor conformers. Thus the Boltzmann-averaged calculated ECD spectra were in line with the B3LYP *in vacuo* results (Figure S38) verifying the absolute configuration of (–)-**26** as 7*R*.

In addition to the new natural products discussed above, 23 known compounds were also isolated. By comparison of their NMR and mass data with the literature,

they were identified as AGI-B4 (**3**),¹⁶ huperxanthone C(**4**),²⁶ pinselin (**5**),¹⁵ sydowinin B (**6**),²⁷ 13-*O*-acetylsydowinin B(**7**),²⁸ 2,11-dihydroxy-1-methoxycarbonyl-9-carboxylxanthone(**8**),²⁹ sydowinin A (**9**),^{26,30} 8-(methoxycarbonyl)-1-hydroxy-9-oxo-9*H*-xanthene-3-carboxylic acid (**10**),³¹ methyl-3,8-dihydroxy-6-methyl-9-oxo-9*H*-xanthene-1-carboxylate (**11**),³² sydowic acid (**12**),³³ sydonic acid (**13**)¹⁷, 11-hydroxysydonic acid (**14**)¹⁸, violaceol I (**17**),³⁴ violaceol II (**18**),³⁴ diorcinol (**19**),³⁴ rikuzenol (**20**)³⁵, lumichrome (**22**),³⁶ WIN 64821 (**23**),³⁷ scopularide A (**24**),¹² and scopularide B (**25**),¹² pyrenochaetic acid A (**27**),²⁰ 7-hydroxy-2,5-dimethylchromone (**28**)³⁸ and ergosterol (**29**).³⁹ It is worth to note that with the exception of the cyclodepsipeptides that had previously been reported from the genus *Scopulariopsis*, the remaining compounds which were identified in this study are reported here for the first time for this genus. Interestingly, we also isolated sydowinin B (**6**) and 11-hydroxysydonic acid (**14**) from the extract of host coral *Stylophora* sp., suggesting that production of structurally similar compounds by *Scopulariopsis* sp. as found in this study may also take place when the fungus is confined within its host.

All compounds (**1–29**) were tested for their cytotoxicity, by examining their effects on the growth of the murine lymphoma cell line (L5178Y) using the MTT method. The xanthone derivative AGI-B4 (**3**), the cyclic depsipeptide scopularide A (**24**), and the phenyl ethers violaceols I and II (**17** and **18**) displayed significant cytotoxicity with IC₅₀ values of 1.5, 1.2, 9.5 and 9.2 μ M, respectively, similar to that of the positive control kahalalide F (IC₅₀ 4.3 μ M), while the remaining compounds exhibited no activity (IC₅₀>15 μ M). The cytotoxicity of AGI-B4 (**3**) and the lack of activity observed for the remaining xanthone derivatives (**1–2**, **4–11**), indicated that both the dihydroxanthone nucleus and a free hydroxyl group at C-12 are structural features that are important for the cytotoxic activity of the analyzed xanthenes.

Comparison of the cytotoxicity between scopularide A (**24**) and B (**25**) suggested that the length of the aliphatic side chain and hence probably the lipophilicity are also important for the cytotoxicity. Moreover, regarding the isolated biphenyl ether derivatives, the cytotoxicity of violaceols I and II (**17** and **18**) and no detectable activity for **19**, led to the assumption that increasing the number of hydroxy groups in these molecules enhanced the cytotoxic activity.

3. Experimental section

3.1. General experimental procedures

Optical rotations were measured on a Perkin-Elmer-241 MC polarimeter. ^1H , ^{13}C and 2D NMR spectral data were recorded in deuterated solvents on Bruker ARX 300 or Avance DMX 600 NMR spectrometers. Mass spectra were obtained on a LC-MS HP1100 Agilent Finnigan LCQ Deca XP Thermoquest and high-resolution mass (HRESIMS) spectra were measured on a FTIRMS-Orbitrap (Thermo Finnigan) mass spectrometer. HPLC analysis was performed with a Dionex Ultimate 3000 LC system coupled with a photodiode array detector (UVD340S), with detection wavelengths of 235, 254, 280 and 340 nm. The separation column (125 x 4 mm, L x ID) was prefilled with Eurospher-10 C₁₈ (Knauer, Germany), whereas the following gradient was used (MeOH, 0.01% HCOOH in H₂O): 0 min, 10% MeOH; 5 min, 10% MeOH; 35 min, 100% MeOH; 45 min, 100% MeOH, with a flow rate of 1 mL/min. Semi-preparative HPLC separation was performed on a semi-preparative RP-HPLC system of LaChrom-Merck Hitachi (pump: L7100 and UV detector L7400; column: Eurospher 100 C₁₈, 300 x 8 mm, Knauer, Germany) with a flow rate of 5.0 mL/min. Routine normal phase column chromatography was performed using Merck MN Silica gel 60 M (0.04–0.063 mm) or Sephadex LH-20 as stationary phases. TLC analyses and preparative TLC were performed on precoated Silica Gel 60 F254 plates (Merck,

Darmstadt, Germany) followed by detection under UV at 254 and 365 nm or after spraying with anisaldehyde reagent or methanol-sulphuric acid (95:5), respectively. Solvents were distilled before use and spectroscopic grade solvents were used for spectroscopic measurements.

3.2. Fungal material

The fungal strain *Scopulariopsis* sp. was isolated from the fresh crushed inner tissues of the Red Sea hard coral *Stylophora* sp. as described previously.⁴⁰ The coral was collected in November 2012 near the coastline of Ain El-Sokhna area, Red Sea, Egypt, and identified as *Stylophora* sp.. A voucher specimen (code ST-1112) was deposited at the Department of Pharmacognosy, Faculty of Pharmacy, Ain-Shams University, Cairo, Egypt. For isolation of fungi the coral sample was thoroughly cleaned with distilled water, then surface sterilization was done with 70% ethanol for 2 min, followed by rinsing with sterile water. To exclude the presence of surface-adhered fungi, an imprint of the coral surface on biomalt agar was performed. The coral pieces were then aseptically crushed and homogenized. Small tissue samples from the inside of the coral were cut aseptically using a sterile blade and pressed onto malt agar plates containing the antibiotic chloramphenicol to suppress bacterial growth (composition of isolation medium: 15 g/L malt extract, 15 g/L agar, and 0.2 g/L chloramphenicol in distilled water, pH 7.4–7.8, adjusted with 10% NaOH or 36.5% HCl). After incubation at room temperature (25°C), the fungal strain under investigation was found to grow exclusively out of the coral tissue, but not on control plates (imprints from the coral surface). From growing cultures, a pure fungal strain (ST-F1) was isolated by repeated reinoculation on fresh malt agar plates.

3.3. Identification of the fungal strain

The fungus was identified using a molecular biological protocol by DNA amplification and sequencing of the ITS region (GenBank accession no: KP027401) as described previously.⁴⁰ This fungal strain was identified as *Scopulariopsis* sp.. A voucher strain is kept in the Institute of Pharmaceutical Biology and Biotechnology, Heinrich-Heine University, Düsseldorf, Germany, with the ID code (ST-F1).

3.4. Cultivation, extraction and isolation

Mass growth of the fungus for the isolation and identification of secondary metabolites was performed in Erlenmeyer flasks (1L each). The fungus was cultivated on solid rice medium (100 g rice and 110 mL water, which was kept overnight before being autoclaved for 20 min at a temperature of 121 °C) in 10 Erlenmeyer flasks (1 L each) for four weeks under static conditions at 25° C.

Each flask of the fungal culture on solid rice medium was extracted three times with 600 mL EtOAc. After combining the extracts and evaporation of EtOAc, partitioning was done for the residue (15 g) between *n*-hexane and 90% aqueous methanol. Evaporation of the 90% methanol fraction gave 10 g, which was fractionated by vacuum liquid chromatography (VLC) on silica gel using a gradient elution of *n*-hexane/EtOAc (100:0 to 0:100) and CH₂Cl₂/MeOH (100:0 to 0:100), where an eluting volume of 500 mL was used for each step. Elution started with *n*-hexane/ethyl acetate gradient in 20% steps, and when 60% *n*-hexane was reached, 10% steps were employed till 100% EtOAc, then DCM/MeOH gradient was applied in 20% steps till 100% MeOH, yielding fourteen fractions (STFV1-V14).

Crystallization of the 40% EtOAc VLC fraction STFV3 (800 mg) afforded white crystals of **29** (28 mg). The remaining supernatant STFV3F (740 mg) was chromatographed on a Sephadex LH-20 column (100 x 5 cm) using 100% MeOH as eluting solvent and similar fractions were combined using TLC analysis to afford **19**

(3 mg). Fraction STFV4 which was eluted from the VLC with 60% EtOAc (235 mg), was further purified using a Sephadex LH-20 column (80 x 4 cm) with 100% MeOH to give **11** (2.5 mg). Fraction STFV5 (545 mg) which was eluted with 80% EtOAc, was chromatographed over a Sephadex LH-20 column (100 x 5 cm) using 100% MeOH as eluent to give 10 subfractions coded STFV5S1 to S10. STFV5S4 (18 mg) was further purified using semi-preparative RP-HPLC with 58% MeOH as eluting system to afford **28** (1.3 mg) and **13** (1 mg). Meanwhile, STFV5S5 (125 mg) was subjected to a Sephadex LH-20 column (70 x 4 cm), using DCM-MeOH (1:1) as mobile phase to yield **17** (6.5 mg), **18** (6 mg), **1** (1.2 mg), **7** (8.2 mg) and **5** (1.8 mg). STFV5S8 (16 mg) was subjected to purification by semi-preparative RP-HPLC using 52% aqueous MeOH to recover **20** (1.8 mg). Fraction STFV6 (365 mg) that was eluted with 100% DCM, was subjected to a Sephadex LH-20 column (100 x 5 cm) eluting with DCM-MeOH (1:1). Fractions were combined according to their TLC profiles into 8 subfractions (STFV6S1 to S8). Subfraction STFV6S5 (18.5 mg) was further purified by semi-preparative HPLC with a gradient of MeOH/H₂O to yield **16** (0.9 mg) and **2** (1.0 mg) at 46% and 61% MeOH, respectively. Similarly, the VLC fraction STFV7 (25% MeOH, 1.82 g) was re-fractionated over a VLC column as previously described, yielding 14 different subfractions (STFV7V1 to V14). The subfraction STFV7V3 (380 mg) was chromatographed over a Sephadex LH-20 column (100 x 5 cm) with 100% MeOH to obtain five pure compounds **14** (14 mg), **3** (8 mg), **22** (0.9 mg), **9** (1.3 mg) and **6** (12 mg). Subfraction STFV7V4 (180 mg) was subjected to a Sephadex LH-20 column (70 x 4 cm) using 100% MeOH as eluent to afford **26** (0.5 mg) and **12** (8 mg). STFV7V6 (1.3 g) was subjected to an additional VLC column as described before, giving 12 subfractions (STFV7V6V1 to V12), where subfraction STFV7V6V5 (380 mg) was chromatographed over a Sephadex LH-

20 column (100 x 5 cm) using 100% MeOH as elution to give 8 subfractions (STFV7V6V5S1 to S8). Purification of the resulting subfraction STFV7V6V5S2 (60 mg) using semi-preparative HPLC with 85% MeOH afforded **25** (8.2 mg) and **24** (40.5 mg) and purification of subfraction STFV7V6V5S6 (18 mg) using semi-preparative HPLC with 69% MeOH yielded **23** (1.4 mg). Meanwhile, subfraction STFV7V6V5S7 (32 mg) was subjected to Sephadex LH-20 column chromatography eluting with 100% MeOH to afford **4** (3.5 mg). The combined subfractions (STFV7V6V5S8 to S11, 42.5 mg), were further purified by a Sephadex LH-20 column (50 x 3 cm) using 100% MeOH as eluent to afford **10** (1.2 mg). Combination of subfractions STFV7V7 and STFV7V8 (138 mg), followed by chromatography on a Sephadex LH-20 column (70 x 4 cm) using 100% MeOH, gave **8** (8.8 mg). The VLC fraction STFV8 (98 mg) which was eluted with 40% MeOH, was fractionated over a Sephadex LH-20 column (70 x 4 cm) using 100% MeOH as eluting solvent, leading to 6 subfractions (STFV8S1 to S6). Further purification of the subfraction STFV8S4 using semi-preparative HPLC using 42% MeOH afforded **15** (1.8 mg). VLC fraction STFV9 (23 mg), which was eluted with 60% MeOH, was directly subjected to semi-preparative HPLC with 53% MeOH as eluting solvent to afford **21** (1.8 mg). Finally, fraction STFV10 (128 mg) eluted with 80% MeOH, was fractionated over a Sephadex LH-20 column (70 x 4 cm) using 100% MeOH as an eluent, resulting in 6 subfractions (STFV10S1 to S6), where the third subfraction STFV10S3 was further purified by semi-preparative HPLC with 55% MeOH to yield **27** (1.1 mg).

3.4.1. 12-Dimethoxypinselin (1). Yellow solid; UV (MeOH) λ_{max} : 203, 237, 265 and 380 nm; ^1H and ^{13}C NMR data see Table 1; HRESIMS $[\text{M}+\text{H}]^+$ m/z 361.0915 (calcd. for $\text{C}_{18}\text{H}_{17}\text{O}_8$, 361.0923).

3.4.2. *12-O-Acetyl-AGI-B4 (2)*. Yellow amorphous solid; $[\alpha]_D^{20}$ 0 (*c* 0.16, MeOH); UV (MeOH) λ_{\max} : 213, 269 and 343 nm; 17% ee according to chiral HPLC analysis with Chiralpack IA (4.6×150 mm, 5 μ m, 1.0 ml/min), 2.97 min retention time (t_R) for the first eluting enantiomer and 4.04 min for the second-eluting one; ^1H and ^{13}C NMR data see Table 1; HRESIMS $[\text{M}+\text{H}]^+$ *m/z* 361.0913 (calcd. for $\text{C}_{18}\text{H}_{17}\text{O}_8$, 361.0923).

3.4.3. *(1R,2R)-AGI-B4 (3)*. Yellow amorphous solid; $[\alpha]_D^{20}$ -28.0 (*c* 0.40, MeOH); UV (MeOH) λ_{\max} : 213, 272 and 345 nm; ECD (MeCN, λ [nm] ($\Delta\epsilon$), *c* = 4.91×10^{-5} M): 348 (-2.1), 302 (4.4), 293sh (3.3), 263 (4.6), 237sh (-9.4), 218sh (-11.5), 208sh (-13.9), 202 (-15.5); ESIMS $[\text{M}+\text{H}]^+$ *m/z* 319.

3.4.4. *11,12-Dihydroxysydonic acid (15)*. White amorphous solid; $[\alpha]_D^{20}$ + 4.3 (*c* 0.23, MeOH); UV (MeOH) λ_{\max} : 220, 246 and 302 nm; ECD (MeCN, λ [nm] ($\Delta\epsilon$), *c* = 5.59×10^{-4} M): 298 (0.1), 210 (-0.3); ^1H and ^{13}C NMR data see Table 2; HRESIMS $[\text{M}+\text{Na}]^+$ *m/z* 321.1307 (calcd. for $\text{C}_{15}\text{H}_{22}\text{NaO}_6$, 321.1314).

3.4.5. *1-Hydroxyboivinianic acid (16)*. White amorphous solid; $[\alpha]_D^{20}$ 0 (*c* 0.07, MeOH); UV (MeOH) λ_{\max} : 211, 242 and 299 nm; ^1H and ^{13}C NMR data see Table 2; HRESIMS $[\text{M}+\text{H}]^+$ *m/z* 237.0759 (calcd for $\text{C}_{12}\text{H}_{13}\text{O}_5$, 237.0763).

3.4.6. *Scopulamide (21)*. Yellow amorphous solid; $[\alpha]_D^{20}$ + 21.2 (*c* 0.25, MeOH); UV (MeOH) λ_{\max} : 205, 251 and 299 nm; ^1H and ^{13}C NMR data see Table 3; HRESIMS $[\text{M}+\text{H}]^+$ *m/z* 324.1438 (calcd. for $\text{C}_{16}\text{H}_{22}\text{NO}_6$, 324.1447).

3.4.7. *Scopupyrone (26)*. White amorphous powder; $[\alpha]_D^{20}$ -18.5 (*c* 0.16, MeOH); UV (MeOH) λ_{\max} : 205 and 300 nm; ECD (MeCN, λ [nm] ($\Delta\epsilon$), *c* = 7.37×10^{-4} M): 299 (-0.3), 233 (-0.1), 207 (0.2); ^1H and ^{13}C NMR data see Table 3; HRESIMS $[\text{M}+\text{H}]^+$ *m/z* 227.1277 (calcd for $\text{C}_{12}\text{H}_{19}\text{O}_4$, 227.1283).

3.5. Computational methods

Mixed torsional/low-mode conformational searches were carried out by means of the Macromodel 9.9.223 software⁴¹ using the Merck Molecular Force Field (MMFF) with an implicit solvent model for CHCl₃ applying a 21 kJ/mol energy window. Geometry reoptimizations of the resultant conformers [B3LYP/6-31G(d) level *in vacuo* and B97D/TZVP^{23,25} with PCM solvent model for MeCN] and TDDFT calculations were performed with Gaussian 09⁴² using various functionals (B3LYP, BH&HLYP, PBE0) and the TZVP basis set. ECD spectra were generated as the sum of Gaussians⁴³ with 2400 and 3000 cm⁻¹ half-height width (corresponding to ca. 16 and 20 nm at 260 nm, respectively), using dipole-velocity-computed rotational strengths. Boltzmann distributions were estimated from the ZPVE-corrected B3LYP/6-31G(d) energies in the gas-phase calculations and from the B97D/TZVP energies in the PCM model ones. The MOLEKEL software⁴⁴ package was used for visualization of the results.

3.6. Marfey's reaction

Marfey's reaction was performed to determine the absolute configuration of serine that was present as a substituent in the new compound **21**. To carry out the hydrolysis step, 0.5 mg of **21** was completely dried and dissolved in 1 mL of 6 N HCl, then left in the oven for 24 hours at 110 °C. After cooling and removal of the remaining solvent in the vacuum, 100 μL of Marfey's reagent (N- α -(2,4-dinitro-5-fluorophenyl)-L-alanine amide) (0.1 mg in 100 μL acetone) and 20 μL of 1M NaHCO₃ were added to the residue and then incubated for 1h at 40 °C. After cooling, 10 μL of 2 M HCl was added and mixed to stop the reaction. After freeze-drying overnight, the dried residue was dissolved in 1 mL methanol and then HPLC-MS measurement was conducted along with authentic L- and D-serine (ICN Biomedicals

Inc.) at a concentration of 50 mM each that had been treated in the same way as described above.

3.7. Cytotoxicity assay

Cytotoxicity was tested against the L5178Y mouse lymphoma cell line, using a microplate 3-(4,5-dimethylthiazole-2-yl)-2,5-diphenyl-tetrazolium bromide (MTT) assay as described previously.⁴⁵ All experiments were carried out in triplicate and repeated thrice. The cytotoxic depsipeptide kahalalide F with IC₅₀ of 4.3 μ M was used as positive control and medium containing 0.1% EGMME-DMSO was employed as negative control.

Acknowledgements

A scholarship granted and financed by the Egyptian government (Ministry of High Education) to M.S.E. is gratefully acknowledged. T.K. and A.M. thank the Hungarian National Research Foundation (OTKA K105871) for financial support and the National Information Infrastructure Development Institute (NIIFI 10038) for CPU time. P.P wishes to thank the Manchot Foundation for support.

Supplementary data

UV, HRESIMS, 1D and 2D NMR data for the new compounds (**1**, **2**, **15**, **16**, **21**, and **26**); ECD calculation for compound **26**.

References and notes

1. Bugni, T. S.; Ireland, C. M. *Nat. Prod. Rep.* **2004**, *21*, 143-163.
2. Goldring, W. P. D.; Pattenden, G. *Acc. Chem. Res.* **2006**, *39*, 354-361.
3. Yamada, T.; Iritani, M.; Minoura, K.; Kawai, K.; Numata, A. *Org. Biomol. Chem.* **2004**, *2*, 2131-2135.
4. Cui, C.-B.; Kakeya, H.; Osada, H. *Tetrahedron* **1996**, *52*, 12651-12666.

5. Mayer, A. M.; Glaser, K. B.; Cuevas, C.; Jacobs, R. S.; Kem, W.; Little, R. D.; McIntosh, J. M.; Newman, D. J.; Potts, B. C.; Shuster, D. E. *Trends Pharmacol. Sci.* **2010**, *31*, 255-265.
6. Liu, Y.; Wray, V.; Abdel-Aziz, M. S.; Wang, C.-Y.; Lai, D.; Proksch, P. *J. Nat. Prod.* **2014**, *77*, 1734-1738.
7. Ola, A. R. B.; Debbab, A.; Kurtán, T.; Brötz-Oesterhelt, H.; Aly, A. H.; Proksch, P. *Tetrahedron Lett.* **2014**, *55*, 3147-3150.
8. El Amrani, M.; Lai, D.; Debbab, A.; Aly, A. H.; Siems, K.; Seidel, C.; Schneckeburger, M.; Gaigneaux, A.; Diederich, M.; Feger, D.; Lin, W.; Proksch, P. *J. Nat. Prod.* **2014**, *77*, 49-56.
9. Liu, Y.; Marmann, A.; Abdel-Aziz, M. S.; Wang, C. Y.; Müller, W. E. G.; Lin, W. H.; Mándi, A.; Kurtán, T.; Daletos, G.; Proksch, P. *Eur. J. Org. Chem.* **2015**, 2646-2653.
10. Orfali, R. S.; Aly, A. H.; Ebrahim, W.; Abdel-Aziz, M. S.; Müller, W. E. G.; Lin, W.; Daletos, G.; Proksch, P. *Phytochem. Lett.* **2015**, *11*, 168-172.
11. Hammerschmidt, L.; Aly, A. H.; Abdel-Aziz, M.; Muller, W. E.; Lin, W.; Daletos, G.; Proksch, P. *Bioorg. Med. Chem.* **2015**, *23*, 712-719.
12. Yu, Z.; Lang, G.; Kajahn, I.; Schmaljohann, R.; Imhoff, J. F. *J. Nat. Prod.* **2008**, *71*, 1052-1054
13. Yang, F.; Chen, G. D.; Gao, H.; Li, X. X.; Wu, Y.; Guo, L. D.; Yao, X. S. *J. Asian Nat. Prod. Res.* **2012**, *14*, 1059-1063.
14. Shao, C.-L.; Xu, R.-F.; Wei, M.-Y.; She, Z.-G.; Wang, C.-Y. *J. Nat. Prod.* **2013**, *76*, 779-782.
15. Yamazaki, M.; Okuyama, E. M. I. *Chem. Pharm. Bull.* **1980**, *28*, 3649-3655.

16. Kim, H. S.; Park, I. Y.; Park, Y. J.; Lee, J. H.; Hong, Y. S.; Lee, J. J. *J. Antibiot.* **2002**, *55*, 669-672.
17. Kudo, S.; Murakami, T.; Miyanishi, J.; Tanaka, K.; Takada, N.; Hashimoto, M. *Biosci., Biotechnol., Biochem.* **2009**, *73*, 203-204.
18. Hamasaki, T.; Nagayama, K.; Hatsuda, Y. *Agric. Biol. Chem.* **1978**, *42*, 37-40.
19. Li, X.-D.; Li, X.-M.; Xu, G.-M.; Zhang, P.; Wang, B.-G. *J. Nat. Prod.* **2015**, *78*, 844-849.
20. Sato, H.; Konomi, K.; Sakamura, S. *Agric. Biol. Chem.* **1981**, *45*, 1675-1679.
21. Bhushan, B.; Bruckner, H. *Amino Acids* **2004**, *27*, 231-247.
22. Claydon, N.; Allan, M.; Hanson, J. R.; Avent, A. G. *Trans. Br. Mycol. Soc.* **1987**, *88*, 503-513.
23. Sun, P.; Xu, D.-X.; Mándi, A.; Kurtán, T.; Li, T.-J.; Schulz, B.; Zhang, W. *J. Org. Chem.* **2013**, *78*, 7030-7047.
24. Nicu, V. P.; Mándi, A.; Kurtán, T.; Polavarapu, P. L. *Chirality* **2014**, *26*, 525-531.
25. Grimme, S. *J. Comput. Chem.* **2006**, *27*, 1787-1799.
26. Ma, T.-T.; Shan, W.-G.; Ying, Y.-M.; Ma, L.-F.; Liu, W.-H.; Zhan, Z.-J. *Helv. Chim. Acta* **2015**, *98*, 148-152.
27. Hamasaki, T.; Sato, Y.; Hatsuda, Y. *Biosci., Biotechnol., Biochem.* **1975**, *39*, 2341-2345.
28. Song, X.-Q.; Zhang, X.; Han, Q.-J.; Li, X.-B.; Li, G.; Li, R.-J.; Jiao, Y.; Zhou, J.-C.; Lou, H.-X. *Phytochem. Lett.* **2013**, *6*, 318-321.
29. Sun, Y. L.; Zhang, X. Y.; Zheng, Z. H.; Xu, X. Y.; Qi, S. H. *Nat. Prod. Res.* **2014**, *28*, 239-244.
30. Goddard, M. L.; Mottier, N.; Jeanneret-Gris, J.; Christen, D.; Tabacchi, R.; Abou-Mansour, E. *J. Agric. Food Chem.* **2014**, *62*, 8602-8607.

31. Shao, C.; Wang, C.; Wei, M.; Gu, Y.; Xia, X.; She, Z.; Lin, Y. *Magn. Reson. Chem.* **2008**, *46*, 1066-1069.
32. Hamasaki, T.; Kimura, Y. *Agric. Biol. Chem.* **1983**, *47*, 163-165.
33. Hamasaki, T.; Sato, Y.; Hatsuda, Y. *Agric. Biol. Chem.* **1975**, *39*, 2337-2340.
34. Fremlin, L. J.; Piggott, A. M.; Lacey, E.; Capon, R. J. *J. Nat. Prod.* **2009**, *72*, 666-670.
35. Takenaka, Y.; Tanahashi, T.; Nagakura, N.; Hamada, N. *Chem. Pharm. Bull.* **2003**, *51*, 794-797.
36. Ding, Z.-G.; Zhao, J.-Y.; Yang, P.-W.; Li, M.-G.; Huang, R.; Cui, X.-L.; Wen, M.-L. *Magn. Reson. Chem.* **2009**, *47*, 366-370.
37. Varoglu, M.; Corbett, T. H.; Valeriote, F. A.; Crews, P. *J. Org. Chem.* **1997**, *62*, 7078-7079.
38. Königs, P.; Rinker, B.; Maus, L.; Nieger, M.; Rheinheimer, J.; Waldvogel, S. R. *J. Nat. Prod.* **2010**, *73*, 2064-2066.
39. Wang, F.; Liu, J. *Nat. Prod. Res. Dev.* **2004**, *16*, 204-206.
40. Kjer, J.; Debbab, A.; Aly, A. H.; Proksch, P. *Nat. Protoc.* **2010**, *5*, 479-90.
41. MacroModel, Schrödinger LLC, **2012**. <http://www.schrodinger.com/MacroModel>.
42. Frisch, M. J.; Trucks, G. W.; Schlegel, H. B.; Scuseria, G. E.; Robb, M. A.; Cheeseman, J. R.; Scalmani, G.; Barone, V.; Mennucci, B.; Petersson, G. A.; Nakatsuji, H.; Caricato, M.; Li, X.; Hratchian, H. P.; Izmaylov, A. F.; Bloino, J.; Zheng, G.; Sonnenberg, J. L.; Hada, M.; Ehara, M.; Toyota, K.; Fukuda, R.; Hasegawa, J.; Ishida, M.; Nakajima, T.; Honda, Y.; Kitao, O.; Nakai, H.; Vreven, T.; Montgomery, J. A.; Peralta, J. E. Jr.; Ogliaro, F.; Bearpark, M.; Heyd, J. J.; Brothers, E.; Kudin, K. N.; Staroverov, V. N.; Kobayashi, R.; Normand, J.; Raghavachari, K.; Rendell, A.; Burant, J. C.; Iyengar, S. S.; Tomasi, J.; Cossi, M.;

Rega, N.; Millam, J. M.; Klene, M.; Knox, J. E.; Cross, J. B.; Bakken, V.; Adamo, C.; Jaramillo, J.; Gomperts, R.; Stratmann, R. E.; Yazyev, O.; Austin, A. J.; Cammi, R.; Pomelli, C.; Ochterski, J. W.; Martin, R. L.; Morokuma, K.; Zakrzewski, V. G.; Voth, G. A.; Salvador, P.; Dannenberg, J. J.; Dapprich, S.; Daniels, A. D.; Farkas, O.; Foresman, J. B.; Ortiz, J. V.; Cioslowski, J.; Fox, D. J. Gaussian 09, Revision B.01, **2010**, Gaussian, Inc., Wallingford CT.

43. Stephens, P. J.; Harada, N. *Chirality* **2010**, *22*, 229-233.
44. Varetto, U. MOLEKEL 5.4., **2009**, Swiss National Supercomputing Centre: Manno, Switzerland.
45. Ashour, M.; Edrada, R.; Ebel, R.; Wray, V.; Wätjen, W.; Padmakumar, K.; Müller, W. E. G.; Lin, W. H.; Proksch, P. *J. Nat. Prod.* **2006**, *69*, 1547-1553.